3 × 2 Channel Waveguide Gyroscope Couplers: Theory

WILLIAM K. BURNS, MEMBER, IEEE, AND A. FENNER MILTON

Abstract—**Gyroscope couplers with three input ports and two output ports which can be implemented in a planar geometry are studied theoretically. Using a local normal mode description in the approximation of coupled mode theory, analytic output power expressions are obtained for the 3 × 2 branching waveguide coupler and the 3 × 2 directional waveguide coupler. When optimized, these devices behave identically to each other and to the three-dimensional 3 × 3 coupler [1] from which they are derived.**

I. Introduction

THE use of a 3 × 3 coupler in a fiber optical gyroscope, as demonstrated by Sheem [1], provides a passive approach to the operation of a fiber gyroscope at maximum sensitivity for low rotation rates. The appeal of this device has led to the investigation of approaches by which it could be implemented in a planar geometry [2] so that precision circuits could be fabricated with the techniques of integrated optics. Two such planar implementations have been suggested: a 3 × 2 branching waveguide coupler [Fig. 1(a)], presented here, and a 3 × 2 directional coupler approach [Fig. 1(b)], also suggested by Sheem [3]. Both these devices recognize the requirement of symmetry about a center line in the direction of propagation and the requirement of an input guide separate from the two output guides. They differ from the 3 × 3 coupler, whether three dimensional [1] or planar [2], [3], in that they utilize only two output guides to the fiber loop. The third guide is terminated in the body of the coupler. They differ in precisely how this is accomplished in that the branching coupler only has one interference region while the directional coupler uses two. Both devices utilize a single-mode (3 single-mode arms) three-arm branching or separating waveguide which, to date, has not been theoretically analyzed. A multimode three-arm branch has been reported in [4].

Our purpose in this paper is to provide an approach to the understanding of the three-arm branch and to apply that understanding to the analysis of the 3 × 2 branching coupler and the 3 × 2 directional coupler. Our branch analysis makes use of the coupler symmetry, mentioned above, to reduce the three-arm branch to an equivalent two-arm branch, which is well understood and can be quantitatively described in the abrupt, power-dividing limit [5], [6]. Our analytical approach is to utilize the approximation of coupled mode theory to develop the local normal modes for a set of three coupled waveguides. With the local normal mode description, we can describe both power transfer between local normal modes in the branches and interference between local normal modes in the interference sections. This allows us to write analytic output power expressions for each 3 × 2 coupler. We find, in fact, that when optimized, the two couplers operate identically. We note that Sheem has described the 3 × 2 directional coupler by considering the modes of each individual guiding region and also using coupled mode theory [3]. Although our local normal mode approach gives a theoretically equivalent result, we feel it adds a useful physical picture of the operation of the device. Our analysis of the three-arm branching waveguide will have general utility to the understanding and design of these structures. The application of this result to the 3 × 2 gyroscope couplers provides simple analytic expressions describing output power in terms of fundamental design parameters and will aid in the future design of this class of 3 × 2 couplers.

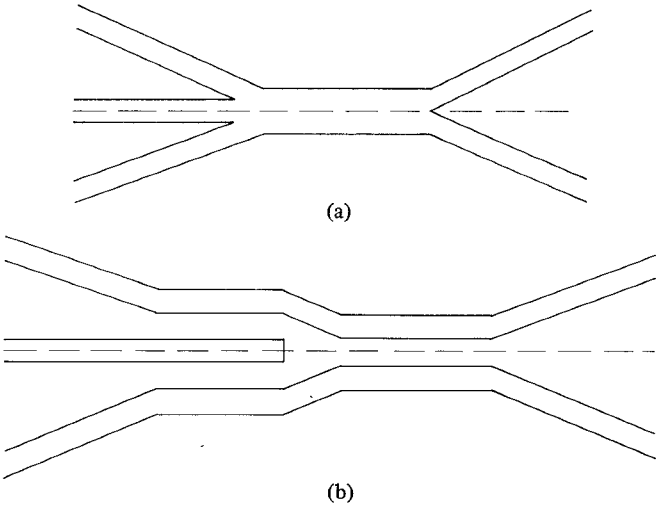

Fig. 1. (a) is a (3 × 2) branching waveguide coupler and (b) is a (3 × 2) directional waveguide coupler [3]. Each device is symmetrical about its center line.

II. Operation of the Three-Arm Branch

In order to treat a three-arm branch we will first develop representations for the local normal modes of the three coupled waveguides of Fig. 2. We assume the outer guides to be identical and equidistant from the center guide. $K_{12}(=K_{23})$ is the nearest neighbor coupling coefficient and K_{13} is the coupling coefficient between the two outer guides. Coupled mode equations describing this system are [7]

$$\frac{da_1}{dz} + i\beta_1 a_1 + i|K_{12}|a_2 + i|K_{13}|a_3 = 0 \tag{1a}$$

$$\frac{da_2}{dz} + i\beta_2 a_2 + i|K_{12}|a_1 + i|K_{12}|a_3 = 0 \tag{1b}$$

$$\frac{da_3}{dz} + i\beta_3 a_3 + i|K_{13}|a_1 + i|K_{12}|a_2 = 0 \tag{1c}$$

where a_1 is the coupled mode amplitude (not local normal mode) and β_1 is the mode propagation constant for guide 1,

Manuscript received March 16, 1982.
The authors are with the Naval Research Laboratory, Washington, DC 20375.

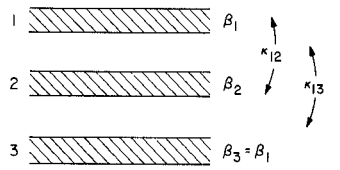

Fig. 2. Three coupled channel waveguides. Guides 1 and 3 are identical and equidistant from guide 2.

etc. When $\beta_3 = \beta_1$, the propagation equations for this three-guide system can be reduced to the equations of the usual two-guide system by the substitution [7]

$$a(z) = a_2(z) \tag{2a}$$

$$b(z) = \frac{1}{\sqrt{2}}\,[a_1(z) + a_3(z)] \tag{2b}$$

to obtain

$$\frac{da}{dz} + i\beta_a a + i|K|b = 0 \tag{3a}$$

$$\frac{db}{dz} + i\beta_b b + i|K|a = 0 \tag{3b}$$

where

$$\beta_a = \beta_2 \tag{4a}$$

$$\beta_b = \beta_1 + |K_{13}| \tag{4b}$$

$$|K| = \sqrt{2}\,|K_{12}|. \tag{4c}$$

One local normal mode of our three coupled waveguides is obtained from the particular solution [7] $a(z) = b(z) = 0$. Substitution into (1) yields the antisymmetric local normal mode, which we denote by the subscript j.

$$A_j(z) = \begin{pmatrix} 1/\sqrt{2} \\ 0 \\ -1/\sqrt{2} \end{pmatrix} \exp^{-i\beta_j z} \tag{5a}$$

where

$$\beta_j = \beta_1 - |K_{13}|. \tag{5b}$$

The column vector in (5a) represents

$$\begin{pmatrix} a_1(0) \\ a_2(0) \\ a_3(0) \end{pmatrix}$$

and has been normalized to unity power.

The two local normal modes for the reduced two-guide system are obtained from the standard normal mode transformation [8], [9] of (3). The result for the local normal mode amplitudes a_i and a_k is

$$a_i(z) = \begin{pmatrix} d \\ e \end{pmatrix} \exp^{-i\beta_i z} \tag{6a}$$

$$a_k(z) = \begin{pmatrix} -e \\ d \end{pmatrix} \exp^{-i\beta_k z} \tag{6b}$$

where the column vector represents

$$\begin{pmatrix} a(0) \\ b(0) \end{pmatrix}.$$

The normal mode propagation constants are

$$\beta_i = \bar{\beta} + |K|\,(X^2 + 1)^{1/2} \tag{7a}$$

$$\beta_k = \bar{\beta} - |K|\,(X^2 + 1)^{1/2} \tag{7b}$$

where

$$\bar{\beta} = \tfrac{1}{2}\,(\beta_a + \beta_b) \tag{8a}$$

$$X = \frac{\Delta\beta}{2|K|} \tag{8b}$$

$$\Delta\beta = \beta_a - \beta_b \tag{8c}$$

and

$$d = \sqrt{\frac{1}{2}\left[1 + \frac{X}{(X^2 + 1)^{1/2}}\right]} \tag{9a}$$

$$e = \sqrt{\frac{1}{2}\left[1 - \frac{X}{(X^2 + 1)^{1/2}}\right]} \tag{9b}$$

so that $d^2 + e^2 = 1$.

By transforming the column vectors in (6) from the reduced two-guide system to the original three-guide system, we obtain the symmetric local normal modes of the three-guide system. We employ (2) at $z = 0$ and maintain the constraint of unity power to obtain from (6)

$$A_i(z) = \begin{pmatrix} e/\sqrt{2} \\ d \\ e/\sqrt{2} \end{pmatrix} \exp^{-i\beta_i z} \tag{10a}$$

$$A_k(z) = \begin{pmatrix} d/\sqrt{2} \\ -e \\ d/\sqrt{2} \end{pmatrix} \exp^{-i\beta_k z}. \tag{10b}$$

These local normal modes have the property $a_1(0) = a_3(0)$ as we would expect from the symmetry of the system.

Power distribution between the center and outer guides in the local normal modes i and k depends on the parameter X [6], [9] which from (4) and (8) can be written as

$$X = \frac{\overline{\Delta\beta} - |K_{13}|}{2\sqrt{2}\,|K_{12}|} \tag{11}$$

where $\overline{\Delta\beta} = \beta_2 - \beta_1$ is the difference in propagation constants for the three coupled guides. For example if $X = 0$, then $d = e = 1/\sqrt{2}$. At large guide separation, $X \to 0$ if $\overline{\Delta\beta} = 0$. However, if $\overline{\Delta\beta} > 0$ then $X \to \infty$, and $d = 1$, $e = 0$. These local normal mode distributions are shown in Fig. 3. This behavior is the analog of the behavior of the two-arm branch for synchronous ($\Delta\beta = 0$) or nonsynchronous ($\Delta\beta \neq 0$) operation [5], [6]. The difference here is that at small guide separation, $\Delta\beta$ becomes a function of guide separation through the coupling coefficient K_{13}.

The utility of the reduced two-guide solution is that we can apply many of the results of the two-arm branch to the three-arm branch. In particular, power transfer between local normal modes at an abrupt transition (case of power division) can be expressed as [9]

$$\frac{|A_{k1}|^2}{|A_{io}|^2} \text{ or } \frac{|A_{i1}|^2}{|A_{ko}|^2} = \frac{(f_o - f_1)^2}{(f_o - f_1)^2 + (1 + f_1 f_o)^2} \tag{12}$$

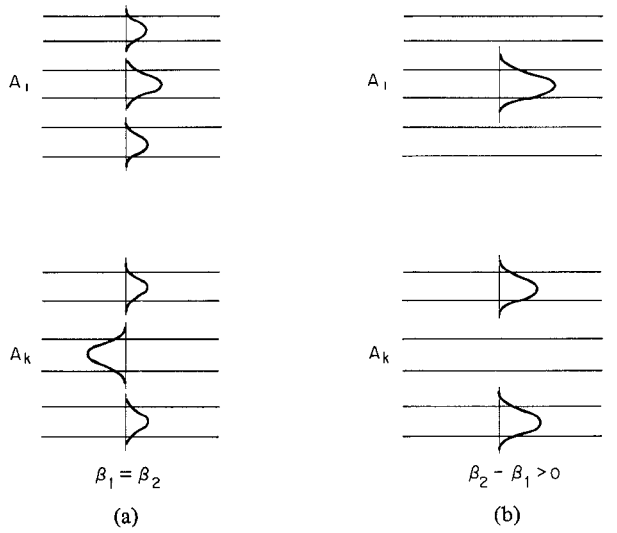

Fig. 3. Shape of the symmetric local normal modes i and k for large guide separation such that the waveguides are uncoupled. (a) Three identical waveguides. (b) Outer waveguides different from center waveguide.

for mode i or k, respectively, incident on the transition, where

$$f = \frac{e}{d} = -X + (X^2 + 1)^{1/2} \tag{13}$$

and o, 1 refer to opposite sides of the transition. We also note that because of the symmetry of our structure, overlap integrals between the antisymmetric mode j and the symmetric modes i and k are always zero. Thus, there is never any power transfer at a transition between j and i or k.

For $\overline{\Delta\beta} > 0$ we typically have a transition between X_o at small or zero guide separation and $X = \infty$ at large guide separation. For input in i, (12) for this case reduces to [6]

$$\frac{|A_{k1}|^2}{|A_{io}|^2} = \frac{1}{2}\left[1 - \frac{X_o}{(X_o^2 + 1)^{1/2}}\right] \tag{14}$$

which is identical to e^2 evaluated at X_o (9b).

As has been discussed in [6], (12) and (14) are derived using coupled mode theory and are accurate in the regime where coupled mode theory is a good approximation. This circumstance occurs when branch arms are well separated (weak coupling) or, in (14), when the reduced two-arm branch is synchronous (small X_o).

III. Operation of the Gyroscope Couplers

We will use the local normal mode formalism developed in Section II for three coupled waveguides to analyze the two types of 3 X 2 gyroscope couplers shown in Fig. 1. For each coupler we envision source input to the center guide on the left of the coupler, the gyroscope fiber loop attached to the two guides on the right, and output signals from the outer guides on the left. Examination of gyroscope output equations [10] indicates that the device will be at the maximum sensitivity or quadrature point when the output signals from the two outer arms are equal for zero rotation. From the normal mode considerations of Section II we can see that, for these couplers, this condition is guaranteed by the requirement for symmetry about the coupler center line. We have a symmetrical excitation or input which will only excite the symmetrical local normal modes i and k. Because of the coupler symmetry, these modes always have equal amplitude in the outside guides. In the absence of rotation there is no coupling to the antisymmetric mode j. Therefore, the output signals must be identical at rest, independent of the mode coupling in the branches and of the lengths of the interference sections. The magnitude of the gyroscope sensitivity at the maximum point, however, will depend on the design of the branches and interference sections, as will be demonstrated below.

We will consider the branching [Fig. 1(a)] or separating (b) waveguide behavior in the abrupt or power dividing limit because it will allow us to superpose modes in a branch while maintaining their relative phase (thereby avoiding a complicated calculation) and because it will allow us to use the analytic expression for power transfer in (14). We are interested in a system of three coupled guides that are not too different in thickness or refractive index profile, so we have a choice of assuming guides with identical propagation constants ($\overline{\Delta\beta} = 0$) or assuming a slight difference in propagation constant between the center and the outer guides ($\overline{\Delta\beta} \neq 0$). We choose the latter case ($\overline{\Delta\beta} \neq 0$) since it represents greater generality, and in fact, turns out to be necessary to optimize the gyroscopic sensitivity of the branching couplers. This represents a significant difference between our analysis and that given in [3] for the 3 X 2 directional coupler.

A. 3 X 2 Branching Coupler

In Fig. 4 we assume $D_1 = D_3 \simeq D_2$ and $D_4 = D_5$, where D_i is the width of channel i. Each channel is single mode so that the central channel of width $2D_4$ supports two normal modes, and the channel at position B of width $2D_1 + D_2$ supports three normal modes. Between B and C the channel width narrows from a three-mode guide to a two-mode guide.

For $\overline{\Delta\beta} > 0$ the local normal modes at large separation (position A) are shown in Fig. 3(b). Input of unity power into guide 2 will excite only local normal mode i, which will travel in the branch and, from (14), convert e^2 of power to mode k by the time it reaches position B [Fig. 4(a)]. The total mode amplitude at B, $\Psi(B)$ is given by the following:

$$\Psi(B) = \sqrt{1 - e^2}\,\Psi_i - e\Psi_k \tag{15}$$

where e is evaluated at B and Ψ_i and Ψ_k represent the transverse field distribution of the symmetric local normal mode amplitudes at B (normalized). In (15) we have inserted the proper phase (π) between Ψ_i and Ψ_k which is apparent from the assumption of power division and the definitions of (10). We assume adiabatic (no power transfer between local normal modes) guide narrowing between B and C so that mode k cuts off with power loss e^2 and mode i evolves without power loss to the mode i of the two-mode guide at C. Mode i then propagates to position D where we assume a symmetric ($\beta_4 = \beta_5$), power dividing two-arm branch leading to each end of the gyro fiber loop. After branch arm separation, mode (not local normal mode) amplitudes in each guiding region are $a_4 = a_5 = \sqrt{(1 - e^2)/2}$. With a total Sagnac phase shift of 2ϕ imposed by the rotating loop, the returns at position E are [Fig. 4(b)]

$$\begin{pmatrix} a_4 \\ a_5 \end{pmatrix} = \sqrt{\frac{1 - e^2}{2}} \begin{pmatrix} \exp^{i\phi} \\ \exp^{-i\phi} \end{pmatrix} \tag{16}$$

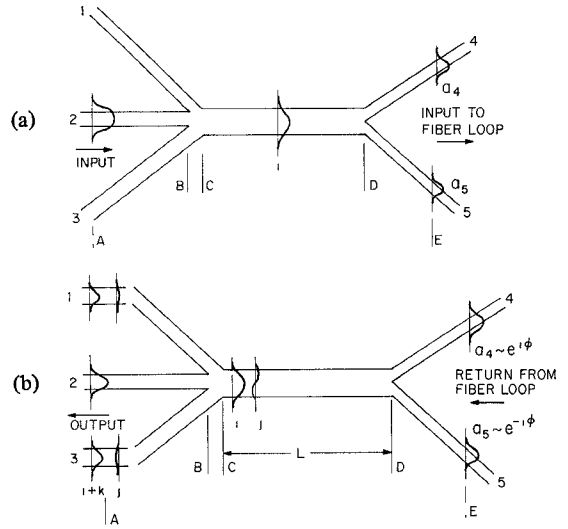

Fig. 4. (a) Input and (b) output mode distributions for the (3 X 2) branching waveguide coupler.

which enter the branch to form a mixture of the symmetric ($i2$) and antisymmetric ($j2$) modes, $\pi/2$ degrees out of phase, of the two-mode structure at D.

$$\Psi(D) = \sqrt{1 - e^2}\,(\cos\phi\Psi_{i2} + i\sin\phi\Psi_{j2}). \tag{17}$$

Here, Ψ_{i2} and Ψ_{j2} represent the transverse field dependence (normalized) of the local normal modes of the two-mode guide. These modes interfere as they propagate to position C

$$\Psi(C) = \sqrt{1 - e^2}\,(\cos\phi\Psi_{i2}\exp^{-i\beta_{i2}L} + i\sin\phi\Psi_{j2}\exp^{-i\beta_{j2}L}) \tag{18}$$

where β_{i2} and β_{j2} are the propagation constants of the local normal modes between C and D, and L is the length of the interference section between C and D. As these modes propagate out the branch to position A, mode i will again transfer e^2 of power to k, while mode j remains uncoupled. The output local normal modes at A are

$$\Psi_i = \sqrt{1 - e^2}\cos\phi\begin{pmatrix}0\\1\\0\end{pmatrix}\exp^{-i\beta_{i2}L} \tag{19a}$$

$$\Psi_j = \sqrt{1 - e^2}\sin\phi\begin{pmatrix}1/\sqrt{2}\\0\\-1/\sqrt{2}\end{pmatrix}\exp^{-i(\beta_{j2}L-\pi/2)} \tag{19b}$$

$$\Psi_k = e\sqrt{1 - e^2}\cos\phi\begin{pmatrix}1/\sqrt{2}\\0\\1/\sqrt{2}\end{pmatrix}\exp^{-i\beta_{i2}L} \tag{19c}$$

where e is to be evaluated at B. The output power in each guide is obtained by superposition of the local normal modes of (19).

$$P_{\substack{1\\3}} = \tfrac{1}{2}(1 - e^2)[1 - (1 - e^2)\cos^2\phi \pm e\cos\alpha\sin 2\phi] \tag{20a}$$

$$P_2 = (1 - e^2)^2\cos^2\phi \tag{20b}$$

where in (20a) the plus sign is taken for P_1 and the minus for P_3, and $\alpha = (\beta_{j2} - \beta_{i2})L - \pi/2$. We define the sensitivity S, assuming unity input power, as

$$S = \left.\frac{dP_1}{d2\phi}\right|_{\phi=0} = \frac{1}{2}(1 - e^2)e\cos\alpha \tag{21}$$

and obtain the maximum sensitivity for the parameter values $e^2(B) = \frac{1}{3}$ and $\alpha = 0$. The 3 X 2 branching coupler is convenient to analyze in that, with the assumption of an abrupt three-arm branch, all the phase shift between the local normal modes occurs in the interference section of length L. From (21) we see that sensitivity is maximized by a $\pi/2$ phase shift in this section, equivalent to the 3 dB coupling required in a 2 X 2 gyroscope coupler. Optimization of the branch design is achieved by maximizing the interference term between local normal modes j and k, $\Psi_j\Psi_k^* + \Psi_j^*\Psi_k$, in the output guide 1 or 3. Mode i plays no role since it has no amplitude in an output guide. The value of X at B required to accomplish this, $e^2(B) = \frac{1}{3}$, is obtained from (14) as

$$X(B) \equiv \frac{\overline{\Delta\beta} - |K_{13}(B)|}{2\sqrt{2}\,|K_{12}(B)|} = \frac{1}{2\sqrt{2}} \tag{22}$$

which in turn requires $\overline{\Delta\beta} = |K_{12}(B)| + |K_{13}(B)|$. Power loss upon input in the coupler is then $\frac{1}{3}$, independent of ϕ. With this optimization the output powers become

$$P_{\substack{1\\3}} = \tfrac{1}{9}(2 - \cos 2\phi \pm \sqrt{3}\sin 2\phi) \tag{23a}$$

$$P_2 = \tfrac{2}{9}(1 + \cos 2\phi). \tag{23b}$$

This result is identical with the corresponding equations (after an equivalent maximization) for the (3 X 3) gyroscope coupler [1], [11]. The maximized coupler sensitivity in both cases is $S = (3\sqrt{3})^{-1}$. Equation (23) is plotted in Fig. 5.

Since detailed knowledge of channel dispersion and coupling coefficients is hard to obtain, it is of interest to estimate the coupler sensitivity for the simplest experimental case of equal branch arm widths $\overline{\Delta\beta} \simeq 0$. We can treat this case with the model developed above by assuming $\overline{\Delta\beta}$ positive, but small compared to $|K_{13}(B)|$. Then at large arm separation $X \to \infty$ and at B we have

$$X(B) \simeq \frac{-|K_{13}(B)|}{2\sqrt{2}\,|K_{12}(B)|}. \tag{24}$$

The coupling coefficients between arms of the branch can be written as [6]

$$|K_{12}| = F_{12}\exp^{-\gamma_{12}x} \tag{25a}$$

$$|K_{13}| = F_{13}\exp^{-\gamma_{13}(2x+D_2)} \tag{25b}$$

where x is a variable separation between arms of the branch, D_2 is the thickness of the center guide, γ_{12} and γ_{13} are transverse momentum components in the cladding region between the channel waveguides, and F_{12} and F_{13} are constants. For our case of very small $\overline{\Delta\beta}$ we have $F_{12} \simeq F_{13}$ and $\gamma_{12} \simeq \gamma_{13} = \gamma$, and as $x \to 0$, (24) for $X(B)$ becomes

$$X(B) \simeq \frac{-\exp^{-\gamma D_2}}{2\sqrt{2}}. \tag{26}$$

For modes near cutoff, we expect the field extent to be large and $\gamma \to 0$ so that $X(B) \to -1/2\sqrt{2}$. For modes far from cutoff, the fields will be well confined so that γD_2 is large and $X(B) \to 0$. We thus expect values of $X(B)$ limited by $-1/2\sqrt{2} \leqslant X(B) \leqslant 0$, depending on waveguide dispersion, for the case of

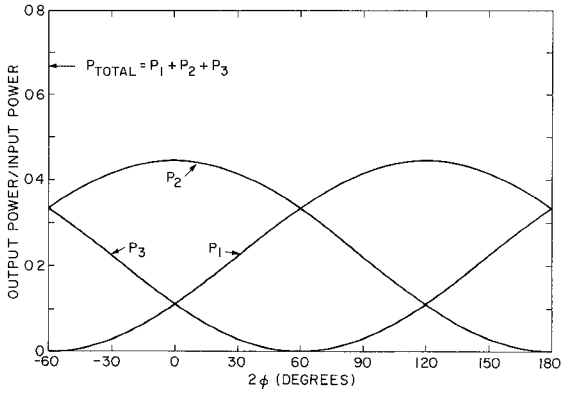

Fig. 5. Channel waveguide output power versus Sagnac phase shift as described by (23). Both the couplers described in this paper are described by this relationship when optimized.

small $\overline{\Delta\beta}$. Corresponding values of e^2 and S are $\frac{2}{3} \leqslant e^2 \leqslant \frac{1}{2}$ and $0.136 \leqslant S \leqslant 0.177$, compared to the optimum sensitivity of $S = 0.192$. Designing the branch with equal arms is then likely to reduce sensitivity between 10 and 30 percent from the optimum value.

B. 3 X 2 Directional Coupler

The 3 X 2 directional coupler of Fig. 6 was suggested by Sheem, who has analyzed it using conventional coupled mode theory which does not use local normal modes [3]. The coupler employs a three-arm separating waveguide and a three-guide interference section (L_1) in place of the branch of the 3 X 2 branching coupler. The two-mode mixing section (L_2) is a directional coupler with nonzero gap. In effect, this device is the directional coupler analog of the 3 X 2 branching coupler. We will analyze the directional coupler under the same assumptions used previously, i.e., $\Delta\beta > 0$ and a symmetrical (power dividing) two-arm branch before the fiber loop.

As before, we input unity power in guide 2 (normal mode i) from the left. In this separating waveguide where the local normal modes are well described by the coupled mode theory developed in Section II on both sides of the branch, power division simply implies that the power distribution at A is reproduced at B. This statement is identical to the assumption of (14), i.e., power transfer of e^2 from i to k in the branch. This equivalence is seen by inspecting the analog of (15) for this case

$$\Psi(B) = d\begin{pmatrix} e/\sqrt{2} \\ d \\ e/\sqrt{2} \end{pmatrix} \exp^{-i\beta_i z} - e\begin{pmatrix} d/\sqrt{2} \\ -e \\ d/\sqrt{2} \end{pmatrix} \exp^{-i\beta_k z} \tag{27}$$

since $d = (1 - e^2)^{1/2}$ and we take $z = 0$ at B. e and d in (27) are evaluated at B. These modes (i and k) interfere between B and C and at C the power in guide 2 is lost. The power in each guide at C is

$$P_1(C) = P_3(C) = (1 - e^2)e^2\,[1 - \cos(\beta_{i3} - \beta_{k3})L_1] \tag{28a}$$

$$P_2(C) = (1 - e^2)^2 + e^4 + 2(1 - e^2)e^2 \cos(\beta_{i3} - \beta_{k3})L_1. \tag{28b}$$

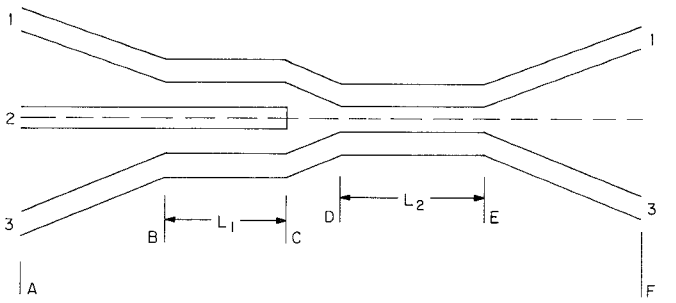

Fig. 6. Detail of the (3 X 2) directional coupler.

We assume the transition between C and D to act as an abrupt (power dividing) transition so that the power in guides 1 and 3 at C is transferred without change to D. This excites normal mode i in the two-guide section between D and E. At D we have

$$\Psi_i(D) = \sqrt{P_1(C)}\begin{pmatrix} 1 \\ 1 \end{pmatrix} \tag{29}$$

where $P_1(C)$ is defined in (28a) and the column vector stands for $\binom{a_1}{a_3}$. The device now behaves identically to the branching coupler discussed in the previous section in that Ψ_i travels to E and divides in the separating branch between E and F.

After traversing the fiber loop the returning Sagnac phase shifted inputs combine in the branch as before to form the normal modes i and j at E, $\pi/2$ out of phase. These modes propagate to D yielding

$$\Psi(D) = \sqrt{P_1(C)}\left[\cos\phi\begin{pmatrix} 1 \\ 1 \end{pmatrix} \exp^{-i\beta_{i2}L_2} + i\sin\phi\begin{pmatrix} 1 \\ -1 \end{pmatrix} \exp^{-i\beta_{j2}L_2}\right] \tag{30}$$

where β_{i2} and β_{j2} denote the normal mode propagation constants in the two-mode section and L_2 is the interference length between D and E. In the abrupt transition between C and D, mode i converts sufficient power to mode k such that at C there is no power in guide 2. We have, then, at C

$$\Psi_{symm}(C) = \sqrt{2P_1(C)}\cos\phi \exp^{-i\beta_{i2}L_2} \cdot \left[e\begin{pmatrix} e/\sqrt{2} \\ d \\ e/\sqrt{2} \end{pmatrix} \exp^{-i\beta_{i3}z} + d\begin{pmatrix} d/\sqrt{2} \\ -e \\ d/\sqrt{2} \end{pmatrix} \exp^{-i\beta_{k3}z}\right] \tag{31a}$$

$$\Psi_j(C) = i\sqrt{P_1(C)}\sin\phi\begin{pmatrix} 1 \\ 0 \\ -1 \end{pmatrix} \exp^{-i\beta_{j2}L_2} \exp^{-i\beta_{j3}z} \tag{31b}$$

where Ψ_{symm} is the sum of i and k, and we assume $z = 0$ at C. These modes then propagate to B where $z = L_1$, and then out the branch to A where power division insures that the power distribution at A is identical to that at B. The output power in each guide at A is

$$P_{\substack{1\\3}} = P_1(C)\,[1 - 2P_1(C)\cos^2\phi \pm \sin 2\phi \cdot \{(1-e^2)\cos[(\beta_{j3} - \beta_{k3})L_1 + \alpha] + e^2\cos[(\beta_{j3} - \beta_{i3})L_1 + \alpha]\}] \quad (32a)$$

$$P_2 = 4P^2(C)\cos^2\phi \quad (32b)$$

where $P_1(C)$ is given by (28a), $\alpha = (\beta_{j2} - \beta_{i2})L_2 - \pi/2$, and e is evaluated at B or C.

Again we wish to maximize the sensitivity $S = dP_1/d2\phi|_{\phi=0}$ which is the coefficient of $\sin 2\phi$ in (32a). Using (4), (5), (7)-(9) we can write the sensitivity, without approximation, as

$$S = \frac{1}{2}\left(1 - \frac{X^2}{X^2+1}\right)\sin^2[\sqrt{2}|K_{12}|(X^2+1)^{1/2}L_1] \cdot \left\{\cos(\delta L_1 + \alpha)\cos[\sqrt{2}|K_{12}|(X^2+1)^{1/2}L_1] - \frac{X}{(X^2+1)^{1/2}}\sin(\delta L_1 + \alpha)\sin[\sqrt{2}|K_{12}|(X^2+1)^{1/2}L_1]\right\} \quad (33)$$

where $\delta = -1/2(\overline{\Delta\beta} + 3|K_{13}|)$ and X is evaluated at B. This coupler is more complicated than the branching coupler considered previously because the local normal modes experience a relative phase shift in the section L_1 as well as in L_2. Thus, we might expect the optimum phase shift in the two-mode section L_2 would not be $\pi/2$ in this case. An inspection of (30) indicates that we can, however, obtain the same sensitivity and output equations for the 3 X 2 directional coupler as we obtained for the branching coupler by choosing parameter values as follows. 1) We choose $\overline{\Delta\beta} = |K_{13}(B)|$ so that $X(B) = 0$ and $\delta = -2|K_{13}(B)|$. 2) Then choose L_1 such that $\sin^2(\sqrt{2}|K_{12}|L_1)\cos(\sqrt{2}|K_{12}|L_1)$ is maximized ($|K_{12}|L_1 = 38.7°$). 3) Finally, choose L_2 such that $\delta L_1 + \alpha \equiv -2|K_{13}(B)| \cdot L_1 + (\beta_{j2} - \beta_{i2})L_2 - \pi/2 = 0$. Then we again have $S = (3\sqrt{3})^{-1}$ and (29) reduces identically to (23) as obtained for the optimized 3 X 2 branching coupler. The optimized parameter values are, however, different for the two cases in that the asymmetry $\overline{\Delta\beta}$ required is smaller for the directional coupler and the length L_2 becomes a function of L_1. Indeed, an experimental choice of equal branch arm widths ($\overline{\Delta\beta} \simeq 0$) will result in an even smaller reduction in sensitivity than was the case for the branching coupler. For example, for $\overline{\Delta\beta} \simeq 0$, a choice of L_1 in (33) such that $|K_{12}|(X^2+1)^{1/2}L_1 = 38.7°$ and L_2 such that $\delta L_1 + \alpha \equiv -\frac{3}{2}|K_{13}|L_1 + (\beta_{j2} - \beta_{i2})L_2 - \pi/2 = 0$ leads to

$$S = \frac{1}{3\sqrt{3}}\left[1 - \frac{1}{(1 + 8\exp^{2\gamma(x+D_2)})}\right] \quad (34)$$

which, following the argument of Section III-A will be within 10 percent of the optimum sensitivity.

IV. Conclusions

We see that, when optimized, both waveguide couplers behave identically to the original three-dimensional 3 X 3 coupler described in [1]. This optimum behavior is characterized by the output (23) and by a sensitivity of $(3\sqrt{3})^{-1}$. An examination of the optimized coupler shows that to obtain the maximum gyroscope sensitivity all these six port couplers (the radiation mode serves as a virtual sixth port in the planar devices) must be adjusted to obtain the same propagation result: 1) the signals from the two output arms are equal for zero Sagnac phase shift, 2) a one-third power loss occurs between input port (2) and the two fiber ports, and 3) for input from a *single* fiber port, an equal division of power occurs between the two output ports (1) and (3). The first condition is satisfied by symmetry around the center line. In the case of the 3 X 2 branching structure the power loss is adjusted by varying the thickness of guide 2 relative to that of guide 1 and 3, thereby changing $\beta_2 - \beta_1$. The third requirement can then be met by varying L. In the case of the 3 X 2 directional coupler the power loss can be optimized by varying L_1 (in this case all input guides can be nearly identical) and then the third requirement met by varying L_2. In practice, the planar structures may not behave exactly as analyzed here, but near optimum performance should be obtained as long as two independent adjustments are possible to meet the requirements described above.

To make these adjustments correctly in a completely passive system would require detailed knowledge of mode dispersion and coupling coefficients in the material system chosen. In an active waveguide system such as Ti:$LiNbO_3$, electrooptic control could be used to adjust the coupling lengths and even vary the asynchronism $(\beta_2 - \beta_1)$ in the branch, although this is more difficult. Thus, a 3 X 2 directional coupler, with two independent electrooptical adjustments, may be easier to fabricate. However, a 3 X 2 branching coupler with a single electrooptical adjustment of the interference length, and equal thickness branch arms, will still operate within 30 percent of the optimum sensitivity.

In the process of treating the 3 X 2 gyroscope couplers, we have developed a local normal mode description for three coupled waveguides which are symmetrical about their center line, and shown, in the coupled mode approximation, how the propagation equations can be reduced to those for two guides. This result can be applied to three-arm branching or separating waveguides with symmetry about a center line, allowing the description of power transfer at a transition.

References

[1] S. K. Sheem, "Fiber-optic gyroscope with [3 X 3] directional coupler," *Appl. Phys. Lett.*, vol. 37, pp. 869-871, Nov. 1980.

[2] S. K. Sheem and W. K. Burns, "Optical fiber gyroscope with (3 X 2) guided wave beam splitter," in *Proc. IOOC 81*, San Francisco, CA, Apr. 1981, paper W13.

[3] S. K. Sheem, "Optical fiber interferometers with [3 X 3] directional couplers: Analysis," *J. Appl. Phys.*, vol. 52, pp. 3865-3872, June 1981.

[4] K. Mitsunaga, K. Murakami, M. Masuda, and J. Koyama, "Optical $LiNbO_3$ 3-branched waveguide and its application to a 4-port optical switch," *Appl. Opt.*, vol. 19, pp. 3837-3842, Nov. 1980.

[5] W. K. Burns and A. F. Milton, "Mode conversion in planar dielectric separating waveguides," *IEEE J. Quantum Electron.*, vol. QE-11, pp. 32-39, Jan. 1975.

[6] W. K. Burns and A. F. Milton, "An analytic solution for mode coupling in optical waveguide branches," *IEEE J. Quantum Electron.*, vol. QE-16, pp. 446-454, Apr. 1980.

[7] A. W. Synder, "Coupled-mode theory for optical fibers," *J. Opt. Soc. Amer.*, vol. 62, pp. 1267-1277, Nov. 1972.

[8] W. H. Louisell, "Analysis of the single tapered mode coupler," *Bell Syst. Tech. J.*, vol. 34, pp. 853–870, July 1955.
[9] A. F. Milton and W. K. Burns, "Mode coupling in tapered optical waveguide structures and electro-optic switches," *IEEE Trans. Circuits Syst.*, vol. CAS-26, pp. 1020–1028, Dec. 1979.
[10] S. C. Rashleigh and W. K. Burns, "Dual-input fiber-optic gyroscope," *Opt. Lett.*, vol. 5, pp. 482–484, Nov. 1980.
[11] The 3 × 3 gyroscope coupler of [1] has a maximum sensitivity at $KL = 40°$.

William K. Burns, for a photograph and biography, see this issue, p. 1588.

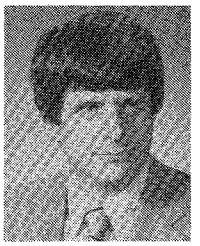

A. Fenner Milton was born in New York, NY, on October 16, 1940. He received the B.A. degree from Williams College, Williamstown, MA, in 1962, and the M.A. and Ph.D. degrees in applied physics, both from Harvard University, Cambridge, MA, in 1963 and 1968, respectively.

He was a technical staff member of the Science and Technology Division, Institute for Defense Analyses when he joined the staff of the Naval Research Laboratory, Washington, DC, as a Consultant to the Optical Sciences Division. In 1977 he became head of the Electro-Optical Technology Branch. His research interests have included photoconductivity, photo emission, nonlinear optics, integrated optics, and infrared focal plane arrays.

Mode Size and Method for Estimating the Propagation Constant of Single-Mode Ti:$LiNbO_3$ Strip Waveguides

STEVEN K. KOROTKY, WILLIAM J. MINFORD, LAWRENCE L. BUHL, MANUEL D. DIVINO, AND ROD C. ALFERNESS

Abstract—**We have formulated a model to calculate the mode size and propagation constant of single-mode titanium-lithium niobate diffused strip waveguides directly from controllable fabrication parameters and basic constants. The model is compared to measurements of the lateral and vertical mode width of Ti:$LiNbO_3$ waveguides for a variety of diffusion conditions. We show that the model accurately predicts the geometrical mean mode size of the two-dimensional waveguide. The model provides a simplified method for estimating the mode size and propagation constant of the guide, and is useful in designing waveguide devices having low fiber/waveguide coupling and bending losses.**

I. Introduction

OPTICAL waveguides produced by the in-diffusion of titanium into lithium niobate crystals have been used to fabricate many electrooptic and acoustooptic devices which are potentially useful for communication and sensing application [1]. The successful construction of some of these devices, directional coupler wavelengths filters [2], for example, depends critically on engineering the propagation constants of the waveguides. For other applications, such as coupling to a fiber [3], it is also necessary to control the size of the waveguide mode. For the most part, research devices based on Ti:$LiNbO_3$ waveguides are developed through trial and error iteration. As devices continue to become increasingly more complex, the need for simple physical models for estimating and relating the mode parameters of Ti:$LiNbO_3$ single-mode strip waveguides becomes more acute.

In this paper, we present measured mode sizes for Ti:$LiNbO_3$ waveguides as a function of several diffusion parameters. We also describe a model, based on the variational principle for the propagation constant, which predicts the characteristics of single-mode diffused strip waveguides in terms of controllable diffusion parameters. The model accurately reproduces the experimental geometrical mean mode size from fundamental parameters, and also provides a simplified method for estimating the propagation constant of diffused strip waveguides.

Manuscript received March 23, 1982; revised May 20, 1982.
S. K. Korotky, L. L. Buhl, M. D. Divino, and R. C. Alferness are with Bell Laboratories, Holmdel, NJ 07733.
W. J. Minford is with Bell Laboratories, Allentown, PA 18103.

II. Experiment

A. Waveguide Fabrication

The waveguides used in the experiments were fabricated on z-cut, y-propagating $LiNbO_3$ crystals having an acoustic grade polish. Waveguide patterns were produced using standard photolithographic techniques. On one crystal, a set of 720 Å thick Ti strips ranging in width from $1\frac{1}{2}$ to 10 μm in $\frac{1}{2}$ μm steps was evaporated. The metal was in-diffused for 6 h at 1100°C. On three other crystals, 6 μm wide Ti strips were prepared with thicknesses of 740, 850, and 1110 Å. The diffusion condition for these crystals was 1050°C for 6 h. In all cases, the diffusion was carried out in an H_2O rich atmosphere to prevent surface guiding due to Li out-diffusion. The ends of the waveguides were blocked and optically polished to achieve flat end surfaces.

B. Mode Profile Measurements

Waveguide mode sizes (full width at half maximum power intensity Γ) in the directions parallel to and perpendicular to the crystal surface were measured for both TE and TM polarizations at the 1.32 μm wavelength using an Nd-YAG laser.

One-dimensional cuts of the 2D-mode profile, which intersect the peak power point, were obtained using a technique similar to that used by Chen and Wang [4] to study mode confinement in semiconductor lasers. The near-field pattern was

0018-9480/82/1000-1784$00.75